



AdS charged black holes in Einstein–Yang–Mills gravity's rainbow: Thermal stability and $P - V$ criticality



Seyed Hossein Hendi ^{a,b,*}, Mehrab Momennia ^a

^a Physics Department and Biruni Observatory, College of Sciences, Shiraz University, Shiraz 71454, Iran

^b Research Institute for Astronomy and Astrophysics of Maragha (RIAAM), P.O. Box 55134-441, Maragha, Iran

ARTICLE INFO

Article history:

Received 21 August 2017

Received in revised form 27 November 2017

Accepted 13 December 2017

Available online 15 December 2017

Editor: N. Lambert

ABSTRACT

Motivated by the interesting non-abelian gauge field, in this paper, we look for the analytical solutions of Yang–Mills theory in the context of gravity's rainbow. Regarding the trace of quantum gravity in black hole thermodynamics, we examine the first law of thermodynamics and also thermal stability in the canonical ensemble. We show that although the rainbow functions and Yang–Mills charge modify the solutions, the first law of thermodynamics is still valid. Based on the phenomenological similarities between the adS black holes and van der Waals liquid/gas systems, we study the critical behavior of the Yang–Mills black holes in the extended phase space thermodynamics. We also investigate the effects of various parameters on thermal instability as well as critical properties by using appropriate figures.

© 2017 The Author(s). Published by Elsevier B.V. This is an open access article under the CC BY license (<http://creativecommons.org/licenses/by/4.0/>). Funded by SCOAP³.

1. Introduction

Black holes are one of the attractive subjects in scientific communities and also the most interesting solutions of the Einstein field equations. In addition to the Schwarzschild and Reissner–Nordström black holes which are, respectively, the vacuum solution and abelian charged solution of Einstein field equations, one can consider non-abelian gauge field as a matter source. One of the most interesting non-abelian gauge theories is the so-called Yang–Mills (YM) field. The motivation for considering the YM field comes from the fact that some string theory models include non-abelian gauge fields into their spectrum and the YM equations have been found in their low energy limit. Indeed, based on the results of superstring models one should find the effects of abelian/non-abelian gauge fields and spinor fields in addition to gravitational fields in the physical phenomena. The first analytic black hole solution of Einstein–YM (EYM) theory was found by Yasskin [1]. Yasskin black hole solution was generalized to higher dimensions by employing the higher dimensional Wu–Yang ansatz [2,3]. In addition, black hole solutions of third order Lovelock gravity coupled to YM field were obtained in Ref. [4,5]. Furthermore, black holes and compact objects have been investigated in a non-abelian Born–Infeld theory [6] and in supersymmetric EYM theories [7]. Non-abelian monopole solutions in asymptotically dS spacetime and black hole hairy solutions coupled to YM field for asymptotically adS spacetime have been obtained in [8] and [9–11], respectively. The Wu–Yang magnetic solutions in YM theory non-minimally coupled to the general relativity have been studied for regular black holes [12,13], wormholes [14,15], and monopoles [16,17]. In the presence of dilaton, the solutions of EYM-dilaton theory have been considered by many authors [18–24]. In addition, black hole solutions in massive gravity coupled to YM gauge field have been investigated in Ref. [25]. These solutions have led to certain revisions of the basic concept of black hole physics based on the no-hair theorem and uniqueness.

Besides, another motivation of non-abelian YM theory comes from the fact that most of string theory classes predict a non-abelian gauge field for unification of gauge-gravity in the high energy regime. In order to unify the general relativity and quantum mechanics, lots of works have been done. In this regard, one can name string theory [26–31], quantum geometry [32], loop quantum gravity [33], spacetime foam models [34], and spacetime discreteness [35]. All these theories have a common feature and when one tries to build up an appropriate theory of quantum gravity, the Lorentz violation will be necessary because the Planck scale is not invariant under the

* Corresponding author.

E-mail addresses: hendi@shirazu.ac.ir (S.H. Hendi), m.momennia@shirazu.ac.ir (M. Momennia).

linear Lorentz transformations. According to the Lorentz violation at the Planck scale, doubly special relativity (DSR) comes into action and modifies the standard energy–momentum dispersion relation as

$$E^2 f^2(\varepsilon) - p^2 g^2(\varepsilon) = m^2 \quad (1)$$

which is known as the modified dispersion relation (MDR). In this equation, $\varepsilon = E/E_P$ is the energy ratio, in which E is the energy of test particle and E_P is the Planck energy. Also, the functions $f(\varepsilon)$ and $g(\varepsilon)$ are called rainbow (energy) functions. It is notable that in the infrared limit, $E \ll E_P$, the rainbow functions reduce to

$$\lim_{\varepsilon \rightarrow 0} f(\varepsilon) = 1, \quad \lim_{\varepsilon \rightarrow 0} g(\varepsilon) = 1, \quad (2)$$

and thus the standard energy–momentum dispersion relation is recovered. There are different classes of MDR which play important role in various branches of physics. For instance, in the context of cosmological and astronomical observations, it was shown that MDR can be responsible for the threshold anomalies of TeV photons and ultra high energy cosmic rays [34,36–40]. In addition, the effect of MDR on the propagation of the observed gravitational wave of the event GW 150914 have been investigated in [41,42]. Also, it was shown that MDR can provide some constraints on the deformations of special relativity and Lorentz violations [43–48].

Following our previous discussion related to DSR, it is worth mentioning that it is an extension of special relativity which is based on two fundamental constants: the velocity of light and the Planck energy. In DSR, the velocity of a test particle not only cannot exceed the speed of light but also its energy cannot be larger than the Planck energy. Nevertheless, DSR is formulated in flat spacetime without considering the gravitational effects. Generalization of DSR to the curved spacetime has been done by Magueijo and Smolin which is called gravity's rainbow [49]. In the context of gravity's rainbow, spacetime is studied with an energy dependent line element, in which such dependency is generally different for the temporal and spatial coordinates. Such an energy dependent spacetime indicates that the particle probing the spacetime can acquire specific range of energies. This will lead to construct a rainbow of energy.

In recent years, there has been a growing interest in gravity's rainbow [50–54]. Wormholes and black hole solutions in different classes have been studied in [55] and [56–60], respectively. Furthermore, it was shown that the gravity's rainbow could remove the big bang singularity in the early universe [61–63]. In addition, a study regarding the hydrostatic equilibrium equation of stars has been investigated in [64]. Also, compact stars in the presence of gravity's rainbow have been studied [65]. Moreover, F(R) theory coupled to gravity's rainbow has been investigated in Ref. [66,67].

In addition to the motivations for studying the gravity's rainbow mentioned above, the basic motivations for considering black holes in the presence of gravity's rainbow are as follows. First, regarding the high energy regime near the black holes, it is required to consider the gravity's rainbow to construct a bridge between general relativity and quantum theory. In other words, the quantum correction of a gravitational system could be observed in an energy dependent spacetime [68–70]. The other motivation comes from the interesting effects of gravity's rainbow on the black hole properties, such as thermodynamics, phase transition, and thermal stability. In addition to previous motivations, the existence of remnants for the black holes [59,71], providing a possible solution toward information paradox [71], modifying uncertainty principle [68,72], furnishing a bridge towards Horava–Lifshitz gravity [73], and being UV completion of Einstein gravity [49] in the presence of gravity's rainbow are the other motivations for considering such an energy dependent spacetime.

In present paper, we are going to study thermal stability and phase transition of EYM black holes in the presence of gravity's rainbow. In the next section, we introduce the field equations of EYM theory in the presence of cosmological constant in 4-dimensional spacetime. Then, we obtain EYM solutions and investigate their geometrical properties. After that, we will calculate the conserved and thermodynamic quantities of the black holes and check the validity of the first law of thermodynamics in Sec. 3. Section 4 is devoted to study the thermal stability of the solutions by using the heat capacity. In Sec. 5, we study the $P - V$ criticality of black holes through extended phase space. We finish our paper with some concluding remarks.

2. Basic field equations and black hole solutions

The four dimensional action of EYM theory in the presence of Maxwell electrodynamic field and cosmological constant is

$$\mathcal{I}_G = -\frac{1}{16\pi} \int_{\mathcal{M}} d^4x \sqrt{-g} (R - 2\Lambda - \mathcal{F}_M - \mathcal{F}_{YM}), \quad (3)$$

where R and Λ are, respectively, the scalar curvature and cosmological constant. Also, $\mathcal{F}_M = F_{\mu\nu} F^{\mu\nu}$ and $\mathcal{F}_{YM} = \text{Tr} \left(F_{\mu\nu}^{(a)} F^{(a)\mu\nu} \right)$ are the Maxwell invariant and the YM invariant, respectively. Varying the action (3) with respect to the metric tensor $g_{\mu\nu}$, the Faraday tensor $F_{\mu\nu}$, and the YM tensor $F_{\mu\nu}^{(a)}$, one can obtain the following field equations

$$G_{\mu\nu} + \Lambda g_{\mu\nu} = T_{\mu\nu}^M + T_{\mu\nu}^{YM}, \quad (4)$$

$$\nabla_\mu F^{\mu\nu} = 0, \quad (5)$$

$$\hat{D}_\mu F^{(a)\mu\nu} = \nabla_\mu F^{(a)\mu\nu} + f_{(b)(c)}^{(a)} A_\mu^{(b)} F^{(c)\mu\nu} = 0, \quad (6)$$

where $G_{\mu\nu}$ is the Einstein tensor, the symbols $f_{(b)(c)}^{(a)}$'s denote the real structure constants of the 3-parameters YM gauge group $SU(2)$ (which can be calculated by using the commutators of the gauge group generators) and $A_\mu^{(a)}$ is the YM potential. In addition, $T_{\mu\nu}^M$ and $T_{\mu\nu}^{YM}$ are the energy momentum tensor of Maxwell and YM fields which can be written as

$$T_{\mu\nu}^M = -\frac{1}{2}g_{\mu\nu}F_{\rho\sigma}F^{\rho\sigma} + 2F_{\mu\lambda}F_{\nu}^{\lambda}, \quad (7)$$

$$T_{\mu\nu}^{YM} = -\frac{1}{2}g_{\mu\nu}F_{\rho\sigma}^{(a)}F^{(a)\rho\sigma} + 2F_{\mu\lambda}^{(a)}F_{\nu}^{(a)\lambda}. \quad (8)$$

Also, the Faraday tensor $F_{\mu\nu}$ and the YM tensor $F_{\mu\nu}^{(a)}$ can be calculated via their related potentials with the following explicit forms

$$F_{\mu\nu} = \nabla_{\mu}A_{\nu} - \nabla_{\nu}A_{\mu}, \quad (9)$$

$$F_{\mu\nu}^{(a)} = \nabla_{\mu}A_{\nu}^{(a)} - \nabla_{\nu}A_{\mu}^{(a)} + f_{(b)(c)}^{(a)}A_{\mu}^{(b)}A_{\nu}^{(c)}. \quad (10)$$

In order to obtain the static spherically symmetric black hole solutions in gravity's rainbow, we take the following energy dependent metric into account

$$ds^2 = -\frac{k(r)}{f^2(\varepsilon)}dt^2 + \frac{dr^2}{g^2(\varepsilon)k(r)} + \frac{r^2}{g^2(\varepsilon)}(d\theta^2 + \sin^2\theta d\varphi^2), \quad (11)$$

where $k(r)$ is an arbitrary function of radial coordinate which should be determined.

In order to find the electromagnetic field, we use the following radial gauge potential ansatz

$$A_{\mu} = \frac{h(r)}{f(\varepsilon)}\delta_{\mu}^0, \quad (12)$$

which satisfies the Maxwell field equations (5) with the following solution

$$\frac{dh(r)}{dr} = E(r) = \frac{q}{r^2}, \quad (13)$$

where q is an integration constant related to electric charge of the solutions.

To solve the YM field, Eq. (6), we use the magnetic Wu–Yang ansatz of the gauge potential [12,16]. In addition, we consider the position dependent generators $\mathbf{t}_{(r)}$, $\mathbf{t}_{(\theta)}$, and $\mathbf{t}_{(\varphi)}$ of the gauge group instead of the standard generators $\mathbf{t}_{(1)}$, $\mathbf{t}_{(2)}$, and $\mathbf{t}_{(3)}$. The relation between the basis of $SU(2)$ group and the standard basis are

$$\begin{aligned} \mathbf{t}_{(r)} &= \sin\theta \cos\nu\varphi\mathbf{t}_{(1)} + \sin\theta \sin\nu\varphi\mathbf{t}_{(2)} + \cos\theta\mathbf{t}_{(3)}, \\ \mathbf{t}_{(\theta)} &= \cos\theta \cos\nu\varphi\mathbf{t}_{(1)} + \cos\theta \sin\nu\varphi\mathbf{t}_{(2)} - \sin\theta\mathbf{t}_{(3)}, \\ \mathbf{t}_{(\varphi)} &= -\sin\nu\varphi\mathbf{t}_{(1)} + \cos\nu\varphi\mathbf{t}_{(2)}, \end{aligned} \quad (14)$$

and it is straightforward to show that the generators satisfy the following commutation relations

$$[\mathbf{t}_{(r)}, \mathbf{t}_{(\theta)}] = \mathbf{t}_{(\varphi)}, \quad [\mathbf{t}_{(\varphi)}, \mathbf{t}_{(r)}] = \mathbf{t}_{(\theta)}, \quad [\mathbf{t}_{(\theta)}, \mathbf{t}_{(\varphi)}] = \mathbf{t}_{(r)}. \quad (15)$$

Since we are looking for the black hole solutions coupled to Wu–Yang monopole, we take the following gauge field characterized by Wu–Yang ansatz [12,16]

$$A_t^{(a)} = 0, \quad A_r^{(a)} = 0, \quad A_{\theta}^{(a)} = \delta_{(\varphi)}^{(a)}, \quad A_{\varphi}^{(a)} = -\nu \sin\theta \delta_{(\theta)}^{(a)}, \quad (16)$$

where the magnetic parameter ν is a non-vanishing integer. One can show that the YM field equations (6) are satisfied under the choice of (16). Using the YM tensor field (10) and Wu–Yang ansatz (16), one finds that the only non-vanishing component of the YM field is

$$F_{\theta\varphi}^{(r)} = \nu \sin\theta. \quad (17)$$

In order to obtain the metric function $k(r)$, one may use the nonzero components of Eq. (4). Our calculations show that the nonzero components of Eq. (4) can be written as

$$tt \text{ (} rr \text{) - component : } Eq_{tt} = r^2 [rk'(r) + k(r) - 1] + \frac{\Lambda r^4}{g^2(\varepsilon)} + \nu^2 g^2(\varepsilon) + q^2 f^2(\varepsilon) = 0, \quad (18)$$

$$\theta\theta \text{ (} \phi\phi \text{) - component : } Eq_{\theta\theta} = r^3 \left[\frac{r}{2}k''(r) + k'(r) \right] + \frac{\Lambda r^4}{g^2(\varepsilon)} - \nu^2 g^2(\varepsilon) - q^2 f^2(\varepsilon) = 0, \quad (19)$$

where prime denotes d/dr . It is worthwhile to mention that both Eq_{tt} and $Eq_{\theta\theta}$ equations are not independent because the metric function $k(r)$ is the only unknown function in these field equations. After some simplifications, one can find the following relation between Eqs. (18) and (19)

$$Eq_{\theta\theta} = \left(\frac{r}{2} \frac{d}{dr} - 1 \right) Eq_{tt}.$$

Solving Eq. (18), one can find that the metric function $k(r)$ has the following form

$$k(r) = 1 - \frac{m}{r} - \frac{\Lambda r^2}{3g^2(\varepsilon)} + \frac{q^2 f^2(\varepsilon)}{r^2} + \frac{\nu^2 g^2(\varepsilon)}{r^2}, \quad (20)$$

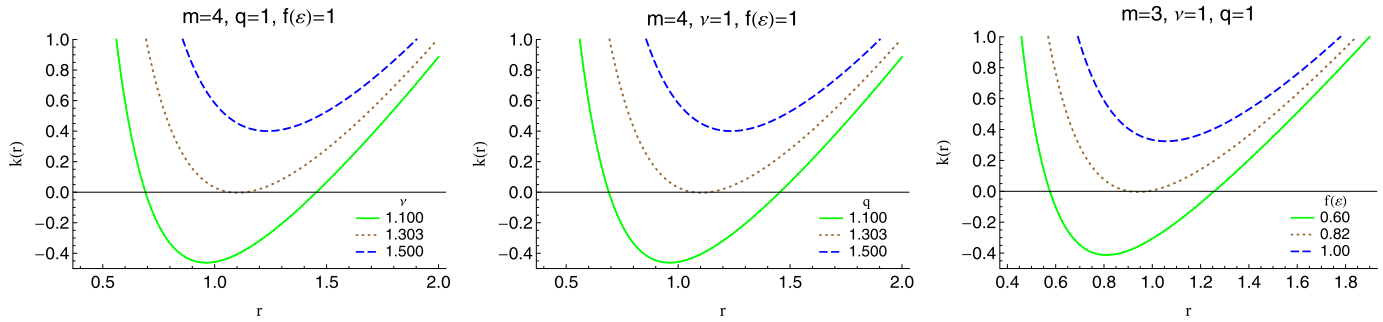


Fig. 1. $k(r)$ versus r for $\Lambda = -1$ and $g(\varepsilon) = 1$. (For interpretation of the colors in this figure, the reader is referred to the web version of this article.)

where m is an integration constant which is related to the total mass of the black hole. It is clear that this metric function satisfies Eq. (19) as well. It is worth mentioning that, for $\nu = 0$, $\Lambda = 0$, and $f(\varepsilon) = 1$ this metric function reduces to the Reissner–Nordström solution, as it should be. In addition, the asymptotical behavior of the solution (20) is adS (or dS) provided $\Lambda < 0$ (or $\Lambda > 0$).

Now, we are going to look for the singularities of the solutions. To do so, one can calculate the Kretschmann scalar as

$$R_{\mu\nu\lambda\kappa}R^{\mu\nu\lambda\kappa} = \frac{8\Lambda^2}{3} + \frac{12g^4(\varepsilon)m^2}{r^6} - \frac{48g^4(\varepsilon)m}{r^7} \left[\nu^2 g^2(\varepsilon) + q^2 f^2(\varepsilon) \right] - \frac{56g^4(\varepsilon)}{r^8} \left[\nu^2 g^2(\varepsilon) + q^2 f^2(\varepsilon) \right]^2, \quad (21)$$

with the following asymptotical behavior

$$\lim_{r \rightarrow \infty} (R_{\mu\nu\lambda\kappa}R^{\mu\nu\lambda\kappa}) = \frac{8\Lambda^2}{3}, \quad \lim_{r \rightarrow 0} (R_{\mu\nu\lambda\kappa}R^{\mu\nu\lambda\kappa}) = \infty, \quad (22)$$

which shows that there is an essential singularity located at $r = 0$. In addition, the Kretschmann scalar reduces to $8\Lambda^2/3$ for large r which confirms that the asymptotical behavior of this spacetime is (a)dS. Moreover, it is clear that this singularity can be covered with a horizon, and therefore, we can interpret the singularity as a black hole (see Fig. 1).

In the coming sections, we will concentrate our attention on the thermodynamic properties of the obtained black hole solutions.

3. The first law of thermodynamics

In this section, we are going to investigate the validity of the first law of thermodynamics. To do so, first, we should calculate the conserved and thermodynamic quantities. Next, we rewrite the total mass as a function of the entropy and electric charge, and then examine the first law of thermodynamics.

Using the surface gravity conception, one can show that the EYM black holes in gravity's rainbow have the following Hawking temperature [60]

$$T = \frac{g(\varepsilon)k'(r)}{4\pi f(\varepsilon)} \Big|_{r=r_+} = \frac{1}{4\pi} \left(\frac{g(\varepsilon)}{f(\varepsilon)r_+} - \frac{\Lambda r_+}{f(\varepsilon)g(\varepsilon)} - \frac{f(\varepsilon)g(\varepsilon)q^2}{r_+^3} - \frac{g^3(\varepsilon)\nu^2}{f(\varepsilon)r_+^3} \right), \quad (23)$$

where r_+ is the largest real positive root of metric function. The electric potential Φ_M , measured at the horizon with respect to infinity as a reference, is given by

$$\Phi_M = \frac{q}{r_+}. \quad (24)$$

Also, using the area law, one can find the entropy of the presented black holes in the following explicit form

$$S = \frac{\pi r_+^2}{g^2(\varepsilon)}. \quad (25)$$

In order to obtain the electric charge of the black hole, we use the flux of the electric field at infinity, yielding

$$Q_M = \frac{qf(\varepsilon)}{g(\varepsilon)}. \quad (26)$$

The ADM (Arnowitt–Deser–Misner) mass of the black hole can be obtained by using the behavior of the metric at large r . The total mass of the black hole is [60]

$$M = \frac{m}{2f(\varepsilon)g(\varepsilon)}, \quad (27)$$

where we can obtain m from $k(r = r_+) = 0$.

Considering Eqs. (23), (25), (26), and (27), one finds that the rainbow functions modify these quantities.

After calculating all the conserved and thermodynamic quantities, we are in a position to check the validity of the first law of thermodynamics. To do this, we use the entropy, electric charge, and mass given by Eqs. (25), (26) and (27), and considering the fact that $k(r = r_+) = 0$, for writing the following Smarr-type formula

$$M(S, Q_M) = \frac{1}{2f(\varepsilon)} \sqrt{\frac{\pi}{S}} \left[\frac{S}{\pi} \left(1 - \frac{\Lambda S}{3\pi} \right) + Q_M^2 + \nu^2 \right]. \quad (28)$$

Considering the parameters Q_M and S as a complete set of extensive parameters, one can define the intensive parameters conjugate to them as the temperature and electric potential

$$T = \left(\frac{\partial M}{\partial S} \right)_{Q_M} = \frac{1}{4\pi f(\varepsilon)} \sqrt{\frac{\pi}{S}} \left[1 - \Lambda S - \frac{\pi}{S} (Q_M^2 + \nu^2) \right], \quad (29)$$

$$\Phi_M = \left(\frac{\partial M}{\partial Q_M} \right)_S = \frac{Q_M}{f(\varepsilon)} \sqrt{\frac{\pi}{S}}. \quad (30)$$

Using Eqs. (25) and (26), one can show that Eqs. (29) and (30) are equal to Eqs. (23) and (24), respectively. Thus, these quantities satisfy the first law of thermodynamics

$$dM = TdS + \Phi_M dQ_M. \quad (31)$$

On the other hand, the black hole also has a global YM charge. In order to find this charge, we use the definition

$$Q_{YM} = \frac{1}{4\pi} \int \sqrt{F_{\theta\varphi}^{(a)} F_{\theta\varphi}^{(a)}} d\theta d\varphi = \nu. \quad (32)$$

In order to enrich the first law of thermodynamics (31), one can consider the YM charge as a thermodynamic variable and introduce an effective YM potential conjugate to it

$$\Phi_{YM} = \left(\frac{\partial M}{\partial Q_{YM}} \right)_{S, Q_M} = \left(\frac{\partial M}{\partial \nu} \right)_{S, Q_M} / \left(\frac{\partial Q_{YM}}{\partial \nu} \right)_{S, Q_M} = \frac{\nu}{f(\varepsilon)} \sqrt{\frac{\pi}{S}} = \frac{g(\varepsilon)}{f(\varepsilon)} \frac{\nu}{r_+}, \quad (33)$$

which satisfies the first law of thermodynamics in a more complete way

$$dM = TdS + \Phi_M dQ_M + \Phi_{YM} dQ_{YM}. \quad (34)$$

4. Thermal stability of the solutions

Here, we are going to study thermal stability of the solutions. For this purpose, we can use the canonical ensemble which leads to studying the heat capacity. The heat capacity related to obtained black hole solutions has the following form

$$C_{Q_M, Q_{YM}} = \frac{T}{\left(\frac{\partial^2 M}{\partial S^2} \right)_{Q_M, Q_{YM}}}, \quad (35)$$

where T is given by Eq. (23). Using Eqs. (25), (26) and (28), it is straightforward to show that

$$\left(\frac{\partial^2 M}{\partial S^2} \right)_{Q_M, Q_{YM}} = \frac{g(\varepsilon)}{8\pi^2 f(\varepsilon) r_+^5} \left\{ -\Lambda r_+^4 - g^2(\varepsilon) r_+^2 + 3g^2(\varepsilon) [q^2 f^2(\varepsilon) + \nu^2 g^2(\varepsilon)] \right\}. \quad (36)$$

In this perspective, the stability condition is based on the sign of heat capacity. The change of sign could happen whether when heat capacity meets root or divergency. The root of heat capacity (or temperature) indicates a bound point which separates physical solutions associated with positive temperature from non-physical ones associated with negative T . On the other hand, the heat capacity divergencies (the roots of Eq. (36)) can be considered as phase transition points. The negativity of the heat capacity represents unstable solutions, whereas its positive value is related to stable state.

Based on above description, one may want to look for the root and divergence points of the heat capacity. The roots of heat capacity, which determine the bound points, are as follows

$$r_{+, BP} = \pm \frac{\sqrt{2\Lambda g(\varepsilon) [g(\varepsilon) + \sqrt{g^2(\varepsilon) - 4\Lambda [q^2 f^2(\varepsilon) + \nu^2 g^2(\varepsilon)]}]}{2\Lambda}, \pm \frac{\sqrt{-2\Lambda g(\varepsilon) [-g(\varepsilon) + \sqrt{g^2(\varepsilon) - 4\Lambda [q^2 f^2(\varepsilon) + \nu^2 g^2(\varepsilon)]}]}{2\Lambda}, \quad (37)$$

which subscript "BP" refers to bound point. At first glance, one may think that it is possible for the heat capacity to have four different roots, but, at most, it has two possible roots. First, in order to have real positive roots, we must consider the following constraint on the solutions

$$g^2(\varepsilon) - 4\Lambda [q^2 f^2(\varepsilon) + \nu^2 g^2(\varepsilon)] > 0. \quad (38)$$

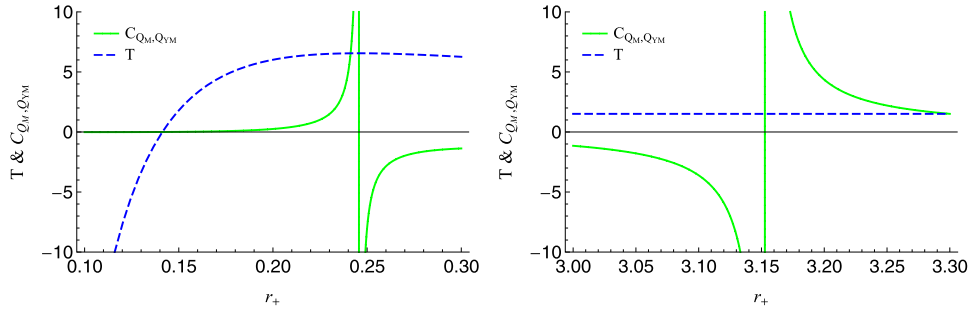


Fig. 2. $C_{Q_M, Q_{YM}}$ and T versus r_+ for $\Lambda = -0.1$, $q = \nu = 0.1$, and $f(\epsilon) = g(\epsilon) = 1$. (For interpretation of the colors in this figure, the reader is referred to the web version of this article.)

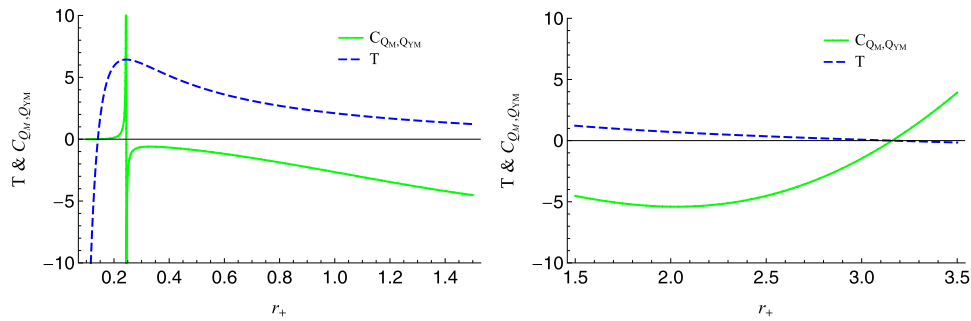


Fig. 3. $C_{Q_M, Q_{YM}}$ and T versus r_+ for $\Lambda = 0.1$, $q = \nu = 0.1$, and $f(\epsilon) = g(\epsilon) = 1$. (For interpretation of the colors in this figure, the reader is referred to the web version of this article.)

Second, one may consider either adS or dS solutions which leads to the following roots

$$r_{+,BP} = \begin{cases} -\frac{\sqrt{-2\Lambda g(\epsilon) \left[-g(\epsilon) + \sqrt{g^2(\epsilon) - 4\Lambda [q^2 f^2(\epsilon) + \nu^2 g^2(\epsilon)]} \right]}}{2\Lambda}, & \text{adS,} \\ \frac{\sqrt{2\Lambda g(\epsilon) \left[g(\epsilon) + \sqrt{g^2(\epsilon) - 4\Lambda [q^2 f^2(\epsilon) + \nu^2 g^2(\epsilon)]} \right]}}{2\Lambda}, \frac{\sqrt{-2\Lambda g(\epsilon) \left[-g(\epsilon) + \sqrt{g^2(\epsilon) - 4\Lambda [q^2 f^2(\epsilon) + \nu^2 g^2(\epsilon)]} \right]}}{2\Lambda}, & \text{dS,} \end{cases} \quad (39)$$

which shows that we have, at most, one (two) root (roots) for adS (dS) spacetime.

On the other hand, divergences of the heat capacity, which determine the phase transition points, are as follows

$$r_{+,DP} = \pm \frac{\sqrt{2\Lambda g(\epsilon) \left[-g(\epsilon) + \sqrt{g^2(\epsilon) + 12\Lambda [q^2 f^2(\epsilon) + \nu^2 g^2(\epsilon)]} \right]}}{2\Lambda}, \pm \frac{\sqrt{-2\Lambda g(\epsilon) \left[g(\epsilon) + \sqrt{g^2(\epsilon) + 12\Lambda [q^2 f^2(\epsilon) + \nu^2 g^2(\epsilon)]} \right]}}{2\Lambda}, \quad (40)$$

which subscript “DP” refers to divergence point. Just like the same procedure that we did for the root points, we should consider

$$g^2(\epsilon) + 12\Lambda [q^2 f^2(\epsilon) + \nu^2 g^2(\epsilon)] > 0 \quad (41)$$

as a constraint on the solutions and extract the divergence points of the heat capacity for both adS and dS solutions as

$$r_{+,DP} = \begin{cases} -\frac{\sqrt{2\Lambda g(\epsilon) \left[-g(\epsilon) + \sqrt{g^2(\epsilon) + 12\Lambda [q^2 f^2(\epsilon) + \nu^2 g^2(\epsilon)]} \right]}}{2\Lambda}, -\frac{\sqrt{-2\Lambda g(\epsilon) \left[g(\epsilon) + \sqrt{g^2(\epsilon) + 12\Lambda [q^2 f^2(\epsilon) + \nu^2 g^2(\epsilon)]} \right]}}{2\Lambda}, & \text{adS,} \\ \frac{\sqrt{2\Lambda g(\epsilon) \left[-g(\epsilon) + \sqrt{g^2(\epsilon) + 12\Lambda [q^2 f^2(\epsilon) + \nu^2 g^2(\epsilon)]} \right]}}{2\Lambda}, & \text{dS.} \end{cases} \quad (42)$$

Although we obtained the roots and divergencies of the heat capacity analytically, but for instance, we plot the temperature and heat capacity in some diagrams to get more insight about the general behavior of the heat capacity (Figs. 2 and 3). We have plotted these figures in different scales and split each diagram into two figures for more clarifications.

Table 1
Asymptotically adS solutions for $\Lambda = -0.1$.

q	ν	$f(\varepsilon)$	$g(\varepsilon)$	Root	Small divergency	Large divergency
0.1000	0.1000	0.5000	1.0000	0.1117	0.1940	3.1563
0.1000	0.1000	0.8000	1.0000	0.1280	0.2224	3.1545
0.1000	0.1000	1.0000	0.5000	0.1115	0.1951	1.5691
0.1000	0.1000	1.0000	0.8000	0.1279	0.2227	2.5200
0.1000	0.1000	1.0000	1.0000	0.1412	0.2456	3.1527
0.0500	0.1000	1.0000	1.0000	0.1117	0.1940	3.1563
0.0100	0.1000	1.0000	1.0000	0.1004	0.1743	3.1574
0.1000	0.0500	1.0000	1.0000	0.1117	0.1940	3.1563
0.1000	0.0100	1.0000	1.0000	0.1004	0.1743	3.1574
0.1000	0.1000	2.0000	1.0000	0.2230	0.3902	3.1381
0.1000	0.1000	3.0000	1.0000	0.3146	0.5564	3.1129
0.1000	0.1000	1.0000	2.0000	0.2234	0.3880	6.3126
0.1000	0.1000	1.0000	3.0000	0.3160	0.5486	9.4709

Table 2
Asymptotically dS solutions for $\Lambda = 0.1$.

q	ν	$f(\varepsilon)$	$g(\varepsilon)$	Small root	Large root	Divergency
0.1000	0.1000	0.5000	1.0000	0.1119	3.1603	0.1933
0.1000	0.1000	0.8000	1.0000	0.1282	3.1597	0.2213
0.1000	0.1000	1.0000	0.5000	0.1121	1.5772	0.1922
0.1000	0.1000	1.0000	0.8000	0.1282	2.5266	0.2210
0.1000	0.1000	1.0000	1.0000	0.1415	3.1591	0.2442
0.0500	0.1000	1.0000	1.0000	0.1118	3.1602	0.1932
0.0100	0.1000	1.0000	1.0000	0.1005	3.1606	0.1738
0.1000	0.0500	1.0000	1.0000	0.1118	3.1602	0.1932
0.1000	0.0100	1.0000	1.0000	0.1005	3.1606	0.1738
0.1000	0.1000	2.0000	1.0000	0.2241	3.1543	0.3844
0.1000	0.1000	3.0000	1.0000	0.3178	3.1462	0.5399
0.1000	0.1000	1.0000	2.0000	0.2237	6.3205	0.3865
0.1000	0.1000	1.0000	3.0000	0.3164	9.4815	0.5468

Form Fig. 2 (adS case), one finds that there are two divergence points and one root located before the small divergence. We recall that the divergencies indicate the phase transition points, whereas the roots of the heat capacity represent bound points. Nevertheless, we have non-physical solutions associated with negative temperature located before the bound point, and the temperature is positive elsewhere. In order to have stable solutions, we should look for the positive heat capacity connected to the positive temperature. Such solutions exist between the bound point and small divergence, and also, after the large divergence. The negative region between two divergencies indicates unstable black holes which may go under a phase transition and become stable ones by losing or absorbing mass. It is worthwhile to mention that such behavior is because of fixed values of $f(\varepsilon)$, $g(\varepsilon)$, q , and ν , and by choosing some different parameters the behavior of the solutions may be totally different.

Considering Fig. 3 (dS case), we find that the heat capacity enjoys two roots and one divergence. There are non-physical solutions before the small root and also after the large root. The only region that enjoys stable and physical solutions is located between the small root and the divergence point. It is worth mentioning that unlike the asymptotically dS solutions, the asymptotically adS black holes with large event horizon are physical and stable. This is one of the reasons that one considers large adS black holes correspond to approximately thermal states in the field theory.

In order to investigate the effect of different parameters on the roots and divergences of the heat capacity, we present Tables 1 and 2. In the case of asymptotically adS solutions, considering Table 1, one finds that both the root and small divergence of the heat capacity are increasing functions of q , ν , and $f(\varepsilon)$, whereas the large divergence is a decreasing function of these parameters. Also, from Table 1 we find that the root and divergence points increase as the rainbow function $g(\varepsilon)$ increases.

It is evident that for dS spacetime, the small root and divergence are increasing functions of q , ν , and $f(\varepsilon)$, whereas we can see the opposite behavior for the large root (Table 2). In addition, as $g(\varepsilon)$ increases, the roots and divergence of the heat capacity increase too.

In addition, we present Figs. 4–7 in order to study the effects of rainbow functions on the bound points and divergencies. These figures have been plotted for Eqs. (39) and (42). From Fig. 4, we can find that the bound point and small divergence are increasing functions of $f(\varepsilon)$, whereas large divergence is a decreasing function of it. As a result, by increasing $f(\varepsilon)$, the region of non-physical and unstable small black holes increases. Therefore, the region of small stable black holes will shift into greater horizon radius until the small divergence disappears (because the small divergence gets complex values for sufficiently large $f(\varepsilon)$). On the other hand, the region of large stable black holes increases until the large divergence disappears. Considering Fig. 5, one finds that both the bound point and large divergence increase as $g(\varepsilon)$ increases too. But the small divergence, first, is a decreasing function of $g(\varepsilon)$ for a very small range, and then it will be an increasing function of this parameter. Figs. 4 and 5 confirm that the divergencies of heat capacity disappear for sufficiently large $f(\varepsilon)$ and/or small $g(\varepsilon)$. In order to find out the reason of the absence of some parts of curves in plotted diagrams, we should investigate the asymptotic behavior of divergencies for large and small rainbow functions. Before starting this matter, we should note that the only bound

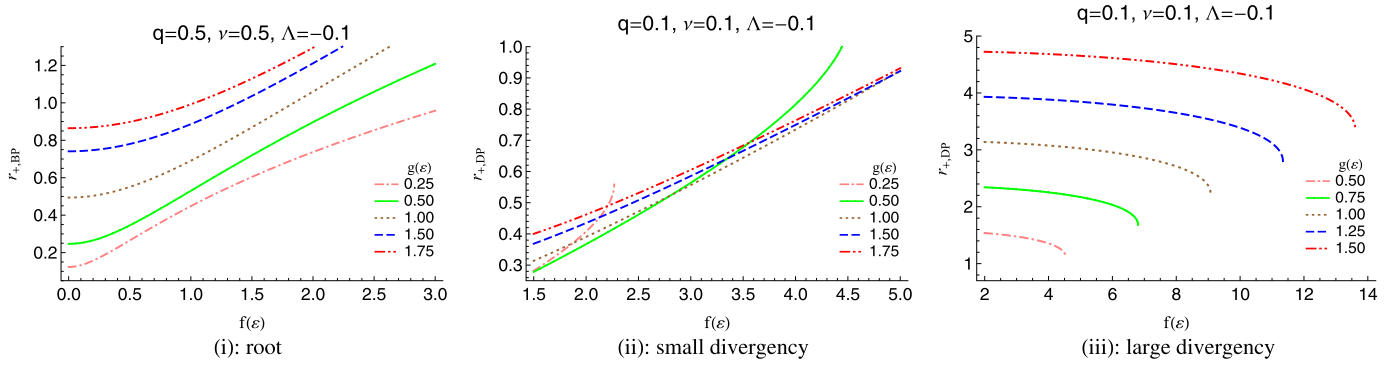


Fig. 4. $r_{+,BP} - f(\epsilon)$ (left) and $r_{+,DP} - f(\epsilon)$ (middle and right) diagrams for adS spacetime. (For interpretation of the colors in this figure, the reader is referred to the web version of this article.)

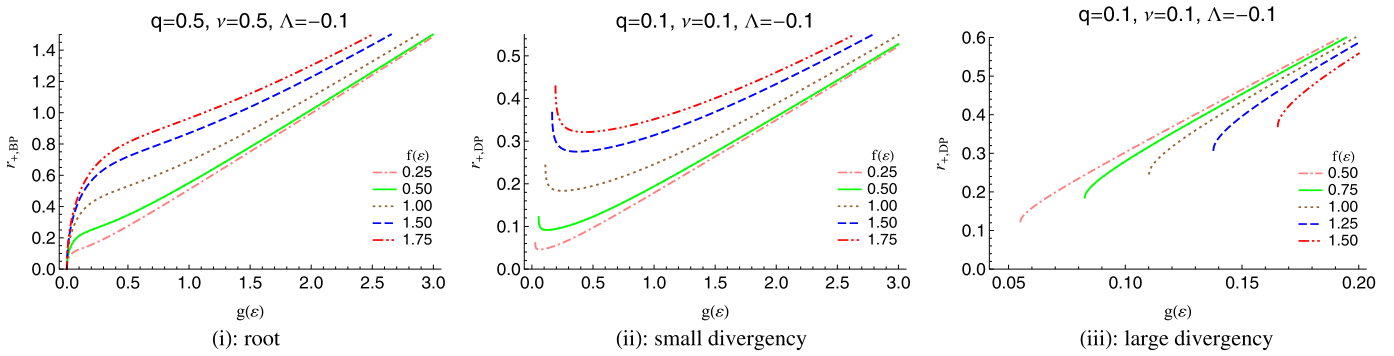


Fig. 5. $r_{+,BP} - g(\epsilon)$ (left) and $r_{+,DP} - g(\epsilon)$ (middle and right) diagrams for adS spacetime. (For interpretation of the colors in this figure, the reader is referred to the web version of this article.)

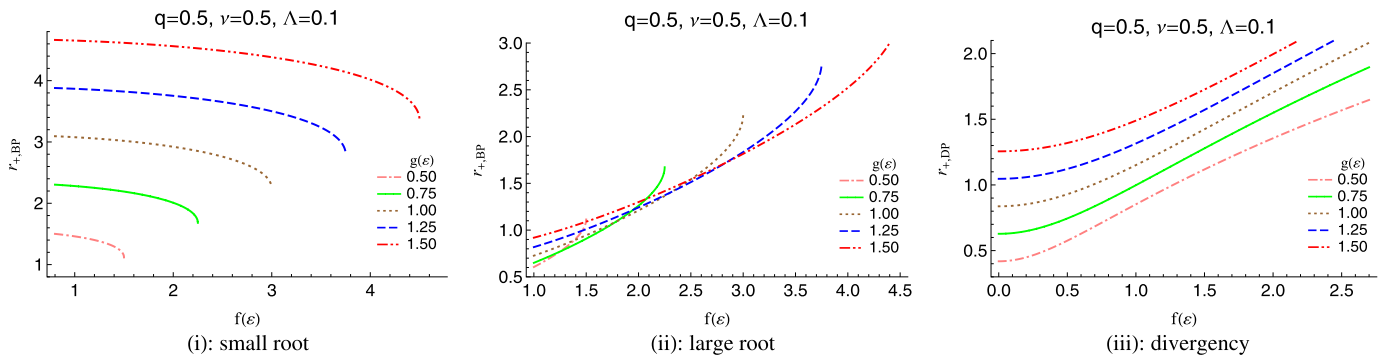


Fig. 6. $r_{+,BP} - f(\epsilon)$ (left and middle) and $r_{+,DP} - f(\epsilon)$ (right) diagrams for dS spacetime. (For interpretation of the colors in this figure, the reader is referred to the web version of this article.)

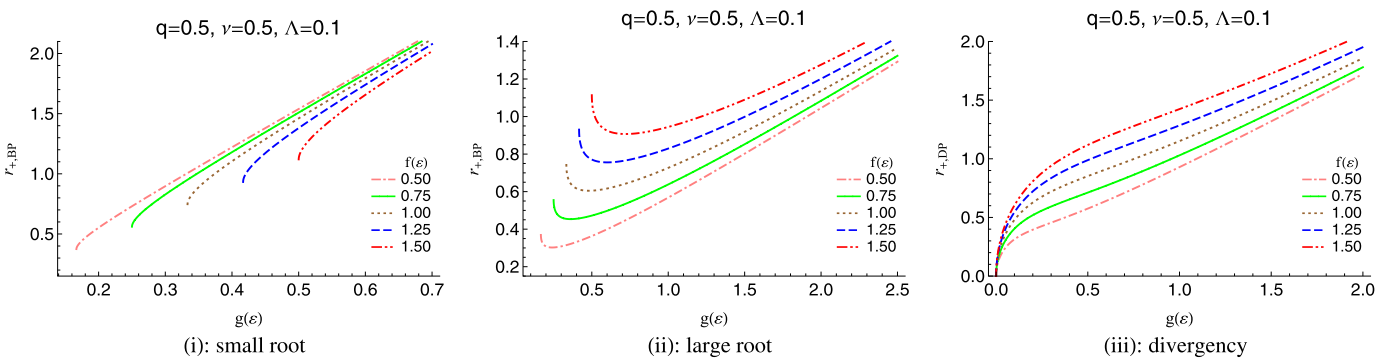


Fig. 7. $r_{+,BP} - g(\epsilon)$ (left and middle) and $r_{+,DP} - g(\epsilon)$ (right) diagrams for dS spacetime. (For interpretation of the colors in this figure, the reader is referred to the web version of this article.)

point of adS solutions is always real and positive (see Eq. (39)). Now, by using the expansion of Eq. (42) for small and large rainbow functions in adS spacetime, we find the following results

$$\text{Small divergency} = \begin{cases} -\frac{\sqrt{2\Lambda g(\varepsilon)\left[-g(\varepsilon)+\sqrt{g^2(\varepsilon)(1+12\Lambda v^2)}\right]}}{2\Lambda} + \mathcal{O}(f^2(\varepsilon)), & \text{small } f(\varepsilon), \\ -\frac{\sqrt{\Lambda f(\varepsilon)g(\varepsilon)\sqrt{3\Lambda q^2}}}{\Lambda} + \mathcal{O}(f^{-1/2}(\varepsilon)), & \text{large } f(\varepsilon), \\ -\frac{\sqrt{\Lambda g(\varepsilon)\sqrt{3\Lambda f^2(\varepsilon)q^2}}}{\Lambda} + \mathcal{O}(g^{3/2}(\varepsilon)), & \text{small } g(\varepsilon), \\ -\frac{\sqrt{2\Lambda(-1+\sqrt{1+12\Lambda v^2})}}{2\Lambda}g(\varepsilon) + \mathcal{O}(g^{-1}(\varepsilon)), & \text{large } g(\varepsilon), \end{cases} \quad (43)$$

where one finds that there is no small divergency for sufficiently large $f(\varepsilon)$ and small $g(\varepsilon)$ (middle panel of Figs. 4 and 5). In addition, in order to have positive real small divergency (for other ranges of rainbow functions), we should obey constraint $0 < 1 + 12\Lambda v^2 < 1$ in addition to Eq. (41), which obviously we followed these conditions in the plotted diagrams (middle panel of Figs. 4 and 5). If one of these conditions violates, the small divergency will disappear for all ranges of both rainbow functions. In addition, one can obtain similar constraints for the large divergency; by using the same procedure, we get

$$\text{Large divergency} = \begin{cases} -\frac{\sqrt{-2\Lambda g(\varepsilon)\left[g(\varepsilon)+\sqrt{g^2(\varepsilon)(1+12\Lambda v^2)}\right]}}{2\Lambda} + \mathcal{O}(f(\varepsilon)), & \text{small } f(\varepsilon), \\ -\frac{\sqrt{-\Lambda f(\varepsilon)g(\varepsilon)\sqrt{3\Lambda q^2}}}{\Lambda} + \mathcal{O}(f^{-1/2}(\varepsilon)), & \text{large } f(\varepsilon), \\ -\frac{\sqrt{-\Lambda g(\varepsilon)\sqrt{3\Lambda f^2(\varepsilon)q^2}}}{\Lambda} + \mathcal{O}(g^{3/2}(\varepsilon)), & \text{small } g(\varepsilon), \\ -\frac{\sqrt{-2\Lambda(1+\sqrt{1+12\Lambda v^2})}}{2\Lambda}g(\varepsilon) + \mathcal{O}(g^{-1}(\varepsilon)), & \text{large } g(\varepsilon), \end{cases} \quad (44)$$

which show that large divergency will be vanished for sufficiently large $f(\varepsilon)$ and small $g(\varepsilon)$ (right panel of Figs. 4 and 5). Besides, large divergency exists only for $1 + 12\Lambda v^2 > 0$, and we followed this condition with (41) in plotted diagrams (right panel of Figs. 4 and 5). It is worthwhile to mention that in order to have both divergence points, we should follow the strong condition, i.e., $0 < 1 + 12\Lambda v^2 < 1$. On the other hand, if one violates $1 + 12\Lambda v^2 > 0$ and/or (41), both divergencies disappear for all ranges of $f(\varepsilon)$ and $g(\varepsilon)$. The presence of Yang–Mills charge in the obtained conditions shows the important effect of magnetic charge on the stability and phase transition of the solutions.

In order to complete our investigation on semi-analytic study of rainbow functions, we focus our attention on asymptotically dS spacetime. The general behavior of roots and divergence point is clear from Figs. 6 and 7. Therefore, we leave this matter due to economic reasons. Equation (42) shows that divergence point is always real and positive. In the case of small root we can write

$$\text{Small root} = \begin{cases} \frac{\sqrt{-2\Lambda g(\varepsilon)\left[-g(\varepsilon)+\sqrt{g^2(\varepsilon)(1-4\Lambda v^2)}\right]}}{2\Lambda} + \mathcal{O}(f(\varepsilon)), & \text{small } f(\varepsilon), \\ \frac{\sqrt{-\Lambda f(\varepsilon)g(\varepsilon)\sqrt{-\Lambda q^2}}}{\Lambda} + \mathcal{O}(f^{-1/2}(\varepsilon)), & \text{large } f(\varepsilon), \\ \frac{\sqrt{-\Lambda g(\varepsilon)\sqrt{-\Lambda f^2(\varepsilon)q^2}}}{\Lambda} + \mathcal{O}(g^{3/2}(\varepsilon)), & \text{small } g(\varepsilon), \\ \frac{\sqrt{-2\Lambda(-1+\sqrt{1-4\Lambda v^2})}}{2\Lambda}g(\varepsilon) + \mathcal{O}(g^{-1}(\varepsilon)), & \text{large } g(\varepsilon), \end{cases} \quad (45)$$

where indicates that there is no small root for large $f(\varepsilon)$ and small $g(\varepsilon)$, and we should follow conditions $0 < 1 - 4\Lambda v^2 < 1$ and (38) to have this small root in dS spacetime. Therefore, we never see this root if one of these conditions violates. In addition, for large root we have

$$\text{Large root} = \begin{cases} \frac{\sqrt{2\Lambda g(\varepsilon)\left[g(\varepsilon)+\sqrt{g^2(\varepsilon)(1-4\Lambda v^2)}\right]}}{2\Lambda} + \mathcal{O}(f(\varepsilon)), & \text{small } f(\varepsilon), \\ \frac{\sqrt{\Lambda f(\varepsilon)g(\varepsilon)\sqrt{-\Lambda q^2}}}{\Lambda} + \mathcal{O}(f^{-1/2}(\varepsilon)), & \text{large } f(\varepsilon), \\ \frac{\sqrt{\Lambda g(\varepsilon)\sqrt{-\Lambda f^2(\varepsilon)q^2}}}{\Lambda} + \mathcal{O}(g^{3/2}(\varepsilon)), & \text{small } g(\varepsilon), \\ \frac{\sqrt{2\Lambda(1+\sqrt{1-4\Lambda v^2})}}{2\Lambda}g(\varepsilon) + \mathcal{O}(g^{-1}(\varepsilon)), & \text{large } g(\varepsilon), \end{cases} \quad (46)$$

where clearly refers to the fact that there is no large root for large $f(\varepsilon)$ and small $g(\varepsilon)$. In addition, there is a constraint $1 - 4\Lambda v^2 > 0$ on the solutions in order to have the large root. The obtained conditions for dS spacetime tell us that if one considers $\Lambda v^2 > 0.25$, both bound points disappear. This shows again the important effect of Yang–Mills charge on the stability of solutions.

In addition to investigation of the rainbow functions effects on the solutions mentioned above, we find that for sufficiently large $f(\varepsilon)$ and small $g(\varepsilon)$ in adS (dS) spacetime, there is no divergency (root). In addition, if one of the conditions $1 + 12\Lambda v^2 > 0$ and (41) ($1 - 4\Lambda v^2 > 0$ and (38)) violates, both divergencies (roots) in adS (dS) spacetime disappear for all ranges of rainbow functions.

5. Extended phase space thermodynamics

Here, we are going to study the $P - V$ criticality of the obtained black holes through extended phase space. The interpretation of the cosmological constant as thermodynamic pressure leads to the van der Waals like behavior and first order phase transition of these black holes. The relation between the cosmological constant and thermodynamical pressure is given by

$$P = -\frac{\Lambda}{8\pi}, \quad (47)$$

where it could be modified in the presence of some modified gravity models. The extensive parameter conjugating to the pressure is thermodynamic volume which could be obtained by

$$V = \left(\frac{\partial H}{\partial P} \right)_{S, Q_M, Q_{YM}}, \quad (48)$$

where H is the enthalpy of system. Here, in the extended phase space, the mass of the black hole plays the role of enthalpy $H \equiv M$ and it is not the internal energy of the system anymore, therefore, the Gibbs free energy is given by $G = H - TS = M - TS$. Using Eqs. (28), (47) and (48), one can obtain the thermodynamic volume as

$$V = \frac{4\pi r_+^3}{3f(\varepsilon)g^3(\varepsilon)}, \quad (49)$$

where we see that the rainbow functions modify the thermodynamic volume.

Now, we are in a position to obtain the Smarr relation in the extended phase space. It is straightforward to show that the following Smarr relation is valid for our solutions

$$M = 2TS - 2PV + Q_M \Phi_M + Q_{YM} \Phi_{YM}, \quad (50)$$

where this modified relation is the Smarr relation of Einstein–Maxwell system with additional YM term as a generalization.

Hereafter, we use r_+ instead of V as a thermodynamic quantity conjugate to pressure, because the thermodynamic volume is a regular function of the event horizon radius (also, one can work with specific volume instead of thermodynamic volume, in which we know that the specific volume is equal to $2r_+$ in natural unite: $c = G = \hbar = 1$ and consequently $l_p = 1$). In order to investigate the van der Waals like behavior of the black holes, we calculate the Gibbs free energy in the following explicit form

$$G = \frac{1}{f(\varepsilon)g(\varepsilon)} \left\{ -\frac{2\pi r_+^3}{3g^2(\varepsilon)} P + \frac{r_+}{4} + \frac{3}{4r_+} [q^2 f^2(\varepsilon) + v^2 g^2(\varepsilon)] \right\}. \quad (51)$$

Now, by using temperature (23) and Eq. (47), we obtain the equation of state, $P(r_+, T)$, for these black holes as

$$P(r_+, T) = \frac{f(\varepsilon)g(\varepsilon)}{2r_+} T - \frac{g^2(\varepsilon)}{8\pi r_+^2} \left\{ 1 - \frac{1}{r_+^2} [q^2 f^2(\varepsilon) + v^2 g^2(\varepsilon)] \right\}. \quad (52)$$

Using the properties of the inflection point

$$\left(\frac{\partial P(r_+, T)}{\partial r_+} \right)_T = \left(\frac{\partial^2 P(r_+, T)}{\partial r_+^2} \right)_T = 0, \quad (53)$$

one can obtain the critical horizon radius, temperature and pressure as

$$r_{+c} = \sqrt{6 [q^2 f^2(\varepsilon) + v^2 g^2(\varepsilon)]},$$

$$T_c = \frac{g(\varepsilon)}{3\pi f(\varepsilon) \sqrt{6 [q^2 f^2(\varepsilon) + v^2 g^2(\varepsilon)]}}, \quad (54)$$

$$P_c = \frac{g^2(\varepsilon)}{96\pi [q^2 f^2(\varepsilon) + v^2 g^2(\varepsilon)]},$$

which lead to the following known near universal ratio

$$\frac{P_c r_{+c}}{T_c} = \frac{1}{4} \left(\frac{3}{4} f(\varepsilon) g(\varepsilon) \right), \quad (55)$$

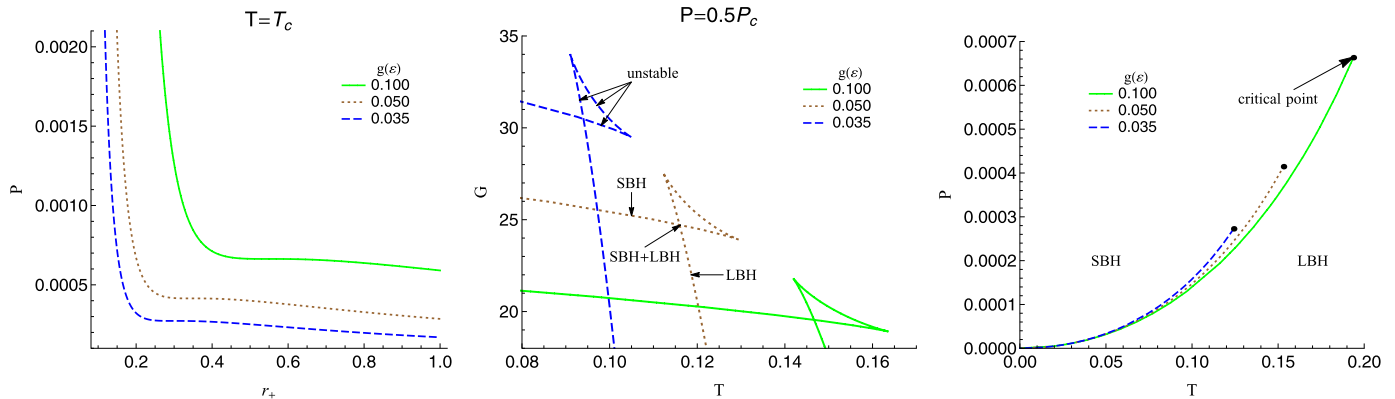


Fig. 8. $P - r_+$, $G - T$, and $P - T$ diagrams for $\nu = 2$, $q = 1$, and $f(\epsilon) = 0.1$. (For interpretation of the colors in this figure, the reader is referred to the web version of this article.)

where shows that the rainbow functions can modify this ratio. For instance, in order to see the general behavior of the obtained black holes, we have plotted $P - r_+$ isotherms, $G - T$ diagrams, and the coexistence lines for special values of different parameters (see Fig. 8).

The presence of both swallow-tail characteristic in $G - T$ diagrams and the inflection point in $P - r_+$ diagrams indicate that obtained black holes undergo a first order phase transition. From Fig. 8, it is clear that as the rainbow function $g(\epsilon)$ increases, the phase transitions are taking place in higher temperature, horizon radius and pressure, but lower Gibbs free energy.

Generally speaking, the van der Waals like phase transition between two different phases is characterized by a swallow-tail shape in $G - T$ diagrams. In case of our solutions, such a behavior represents a phase transition between small and large black holes. The $P - r_+$ isotherm at critical point indicates a second order small/large black hole phase transition (because of vanishing latent heat). The coexistence curve is located between small and large black holes, and terminates at the critical point with $P = P_c$, $T = T_c$, $r_+ = r_{+c}$. There are mixed small-plus-large black holes along the coexistence curve. If one crosses the curve from left to right or top to bottom, the system transforms from small black hole to large black hole. At supercritical temperatures and pressures above T_c and P_c , the small and large black holes are physically indistinguishable and this area is supercritical region.

From Eqs. (54) and (55), one can see the effects of different parameters on the critical points. Considering these equations, it is clear that as the electric charge and YM charge increase, the phase transitions are taking place in higher horizon radius with lower temperature and pressure, but the ratio (55) stays unchanged. Also, the critical horizon radius and $P_c r_{+c}/T_c$ are increasing functions of the rainbow function $f(\epsilon)$, whereas the critical temperature and pressure are decreasing functions of it. As a result, we find that the rainbow functions have significant impact on the critical properties.

6. Conclusions

In this paper, we have obtained EYM black hole solutions with the Maxwell electrodynamics and magnetic Wu–Yang ansatz in the presence of an energy dependent spacetime. We have studied the geometric properties of the solutions and found that there is an essential singularity at the origin which can be covered with an event horizon. In addition, we have calculated the conserved and thermodynamic quantities of the mentioned (a)dS black hole solutions and obtained a Smarr-type formula for the mass as a function of the extensive parameters. We have shown that although the YM theory and gravity's rainbow modify the solutions and their related quantities, the first law of thermodynamics is still hold.

Then, we have investigated thermal stability of the obtained black holes and studied the effects of different parameters on the phase transition and bound points. We have seen that the maximum number of bound points and phase transitions depends on the sign of Λ (consideration of adS or dS spacetime). The maximum number of bound points for asymptotically adS (dS) black holes were one (two), whereas the available maximum number of phase transition points were two (one). Besides, it was shown that there is no divergency (root) for sufficiently large $f(\epsilon)$ and small $g(\epsilon)$ in adS (dS) spacetime. On the other hand, in order to have both divergency (roots) in adS (dS) spacetime for other ranges of rainbow functions, we should follow the conditions $1 + 12\Lambda\nu^2 > 0$ and (41) ($1 - 4\Lambda\nu^2 > 0$ and (38)). Therefore, if one violates one of these conditions, there will not be any divergency (root) for all ranges of rainbow functions. In addition, we have shown that although the large adS black holes are physical solutions, the same behavior is not true for the large dS black holes and they are non-physical solutions. We have obtained two constraints for having bound point and/or phase transition, and therefore, if one violates one of such constraints the heat capacity will never meet any bound point and/or phase transition point. In addition, we have studied the effects of different parameters on both branches of adS and dS solutions.

Furthermore, we have investigated the possibility of existence of van der Waals like phase transition for the obtained adS black hole solutions by considering the negative cosmological constant as an effective dynamical pressure. We have calculated the critical quantities of the black holes analytically, and obtained a modified version of near universal ratio of critical point. We have shown that such black holes can go under a first order phase transition, and therefore, the small/large phase transition does occur. We have found that the YM charge, ν , and the rainbow functions $f(\epsilon)$ and $g(\epsilon)$ modify the critical pressure, P_c , critical horizon radius, r_{+c} , and critical temperature, T_c . In addition, we have shown that, contrary to the contribution of rainbow functions, the YM charge does not have any effect on the near universal ratio $P_c r_{+c}/T_c$.

Finally, it is worth to mention that we have studied the effects of different parameters q , ν , $f(\epsilon)$ and $g(\epsilon)$ on the critical points and collected the results in a couple of appropriate tables. The structure of black holes in the presence of gravity's rainbow is quite different comparing to the EYM theory and its phenomenology is also describing a more general case. Following our results, it is notable that

one can use the obtained black hole solutions and their higher dimensional extension to investigate their dynamic stability, geometrical thermodynamics, entropy spectrum, and quasi normal modes. These extensions are under examination and will be addresses elsewhere.

Acknowledgements

The authors wish to thank the anonymous referee for the constructive comments that enhanced the quality of this paper. We would like to thank Shiraz University Research Council. MM wishes to thank A. Dehyadegari for helpful discussions. This work has been supported financially by the Research Institute for Astronomy and Astrophysics of Maragha, Iran.

References

- [1] P.B. Yasskin, *Phys. Rev. D* 12 (1975) 2212.
- [2] S.H. Mazharimousavi, M. Halilsoy, *Phys. Rev. D* 76 (2007) 087501.
- [3] S.H. Mazharimousavi, M. Halilsoy, *J. Cosmol. Astropart. Phys.* 12 (2008) 005.
- [4] S.H. Mazharimousavi, M. Halilsoy, *Phys. Lett. B* 665 (2008) 125.
- [5] S.H. Mazharimousavi, M. Halilsoy, *Phys. Lett. B* 681 (2009) 190.
- [6] M. Wirschins, A. Sood, J. Kunz, *Phys. Rev. D* 63 (2001) 084002.
- [7] M. Huebscher, P. Meessen, T. Ortin, S. Vaula, J. High Energy Phys. 09 (2008) 099.
- [8] M.S. Volkov, N. Straumann, G. Lavrelashvili, M. Heusler, O. Brodbeck, *Phys. Rev. D* 54 (1996) 7243.
- [9] E. Winstanley, *Class. Quantum Gravity* 16 (1999) 1963.
- [10] J. Bjoraker, Y. Hosotani, *Phys. Rev. Lett.* 84 (2000) 1853.
- [11] J. Bjoraker, Y. Hosotani, *Phys. Rev. D* 62 (2000) 043513.
- [12] A.B. Balakin, J.P.S. Lemos, A.E. Zayats, *Phys. Rev. D* 93 (2016) 024008.
- [13] A.B. Balakin, J.P.S. Lemos, A.E. Zayats, *Phys. Rev. D* 93 (2016) 084004.
- [14] A.B. Balakin, S.V. Sushkov, A.E. Zayats, *Phys. Rev. D* 75 (2007) 084042.
- [15] A.B. Balakin, A.E. Zayats, *Phys. Rev. D* 90 (2014) 044049.
- [16] A.B. Balakin, A.E. Zayats, *Phys. Lett. B* 644 (2007) 294.
- [17] A.B. Balakin, H. Dehnen, A.E. Zayats, *Phys. Rev. D* 76 (2007) 124011.
- [18] G. Lavrelashvili, D. Maison, *Nucl. Phys. B* 410 (1993) 407.
- [19] E.E. Donets, D.V. Galtsov, *Phys. Lett. B* 302 (1993) 411.
- [20] P. Bizon, *Acta Phys. Pol. B* 24 (1993) 1209.
- [21] T. Torii, K. Maeda, *Phys. Rev. D* 48 (1993) 1643.
- [22] Y. Brihaye, E. Radu, *Phys. Lett. B* 636 (2006) 212.
- [23] E. Radu, Y. Shnir, D.H. Tchraikian, *Phys. Rev. D* 75 (2007) 045003.
- [24] M.H. Dehghani, A. Bazrafshan, *Int. J. Mod. Phys. D* 19 (2010) 293.
- [25] K. Meng, J. Li, *Europhys. Lett.* 116 (2016) 10005.
- [26] G. Veneziano, *Europhys. Lett.* 2 (1986) 199.
- [27] E. Witten, *Phys. Today* 49 (4) (1996) 24.
- [28] D. Atami, M. Ciafaloni, G. Veneziano, *Phys. Lett. B* 197 (1987) 81.
- [29] D. Atami, M. Ciafaloni, G. Veneziano, *Phys. Lett. B* 216 (1989) 41.
- [30] D. Atami, M. Ciafaloni, G. Veneziano, *Nucl. Phys. B* 347 (1990) 550.
- [31] K. Konishi, G. Paffuti, P. Provero, *Phys. Lett. B* 234 (1990) 276.
- [32] S. Capozziello, G. Lambiase, G. Scarpetta, *Int. J. Theor. Phys.* 39 (2000) 15.
- [33] L.J. Garay, *Int. J. Mod. Phys. A* 10 (1995) 145.
- [34] G. Amelino-Camalia, J.R. Ellis, N.E. Mavromatos, D.V. Nanopoulos, S. Sarkar, *Nature* 393 (1998) 763.
- [35] G. 't Hooft, *Class. Quantum Gravity* 13 (1996) 1023.
- [36] D. Colladay, V.A. Kostelecky, *Phys. Rev. D* 58 (1998) 116002.
- [37] S.R. Coleman, S.L. Glashow, *Phys. Rev. D* 59 (1999) 116008.
- [38] G. Amelino-Camalia, T. Piran, *Phys. Rev. D* 64 (2001) 036005.
- [39] T. Jacobson, S. Liberati, D. Mattingly, *Phys. Rev. D* 66 (2002) 081302.
- [40] T.A. Jacobson, S. Liberati, D. Mattingly, F.W. Stecker, *Phys. Rev. Lett.* 93 (2004) 021101.
- [41] D. Blas, M.M. Ivanov, I. Sawicki, S. Sibiryakov, *JETP Lett.* 103 (2016) 624.
- [42] M. Arzano, G. Calcagni, *Phys. Rev. D* 93 (2016) 124065.
- [43] R. Aloisio, P. Blasi, P.L. Ghia, A.F. Grillo, *Phys. Rev. D* 62 (2000) 053010.
- [44] R.C. Myers, M. Pospelov, *Phys. Rev. Lett.* 90 (2003) 211601.
- [45] G. Gelmini, S. Nussinov, C.E. Yaguna, *J. Cosmol. Astropart. Phys.* 0506 (2005) 012.
- [46] V. Baukh, A. Zhuk, T. Kahnashvili, *Phys. Rev. D* 76 (2007) 027502.
- [47] S.I. Kruglov, *Phys. Lett. B* 718 (2012) 228.
- [48] A.S. Sefiedgar, K. Nozari, H.R. Sepangi, *Phys. Lett. B* 696 (2011) 119.
- [49] J. Magueijo, L. Smolin, *Class. Quantum Gravity* 21 (2004) 1725.
- [50] R. Garattini, B. Majumder, *Nucl. Phys. B* 884 (2014) 125.
- [51] Z. Chang, S. Wang, *Eur. Phys. J. C* 75 (2015) 259.
- [52] G. Santos, G. Gubitosi, G. Amelino-Camalia, *J. Cosmol. Astropart. Phys.* 08 (2015) 005.
- [53] A.F. Ali, M.M. Khalil, *Europhys. Lett.* 110 (2015) 20009.
- [54] S.H. Hendi, S. Panahiyan, B. Eslam Panah, M. Faizal, M. Momennia, *Phys. Rev. D* 94 (2016) 024028.
- [55] R. Garattini, F.S.N. Lobo, arXiv:1512.04470.
- [56] P. Galan, G.A. Mena Marugan, *Phys. Rev. D* 74 (2006) 044035.
- [57] Y. Gim, W. Kim, *J. Cosmol. Astropart. Phys.* 05 (2015) 002.
- [58] S.H. Hendi, M. Faizal, B. Eslam Panah, S. Panahiyan, *Eur. Phys. J. C* 76 (2016) 296.
- [59] A.F. Ali, *Phys. Rev. D* 89 (2014) 104040.
- [60] S.H. Hendi, S. Panahiyan, B. Eslam Panah, M. Momennia, *Eur. Phys. J. C* 76 (2016) 150.
- [61] A. Awad, A.F. Ali, B. Majumder, *J. Cosmol. Astropart. Phys.* 10 (2013) 052.
- [62] S.H. Hendi, M. Momennia, B. Eslam Panah, M. Faizal, *Astrophys. J.* 827 (2016) 153.
- [63] S.H. Hendi, M. Momennia, B. Eslam Panah, S. Panahiyan, *Phys. Dark Universe* 16 (2017) 26.
- [64] S.H. Hendi, G.H. Bordbar, B. Eslam Panah, S. Panahiyan, *J. Cosmol. Astropart. Phys.* 09 (2016) 013.
- [65] R. Garattini, G. Mandanici, arXiv:1601.00879.
- [66] S.H. Hendi, B. Eslam Panah, S. Panahiyan, M. Momennia, *Adv. High Energy Phys.* 2016 (2016) 9813582.

- [67] A. Chatrabhuti, V. Yingcharoenrat, P. Channuie, *Phys. Rev. D* 93 (2016) 043515.
- [68] Y. Ling, X. Li, H. Zhang, *Mod. Phys. Lett. A* 22 (2007) 2749.
- [69] L. Smolin, *Nucl. Phys. B* 742 (2006) 142.
- [70] R. Garattini, G. Mandanici, *Phys. Rev. D* 85 (2012) 023507.
- [71] A.F. Ali, M. Faizal, M.M. Khalil, *Nucl. Phys. B* 894 (2015) 341.
- [72] H. Li, Y. Ling, X. Han, *Class. Quantum Gravity* 26 (2009) 065004.
- [73] R. Garattini, E.N. Saridakis, *Eur. Phys. J. C* 75 (2015) 343.